ENVIRONMENTAL RESEARCH
LETTERS



OPEN ACCESS

RECEIVED
20 February 2026

REVISED
29 March 2026

ACCEPTED FOR PUBLICATION
1 June 2026

PUBLISHED
12 June 2026



LETTER

# Permafrost carbon–climate feedback amplifies Earth system tipping risks

**Norman J Steinert**[1,2,*], **Gregory Munday**[3], **Marit Sandstad**[1], **Benjamin M Sanderson**[1] and **Nico Wunderling**[2,4,5,*]

[1] CICERO Center for International Climate Research, Oslo, Norway
[2] Earth Resilience Science Unit, Potsdam Institute for Climate Impact Research (PIK), Member of the Leibniz Association, Potsdam, Germany
[3] University of Oxford, Oxford, United Kingdom
[4] Center for Critical Computational Studies (C3S), Goethe University Frankfurt, Frankfurt am Main, Germany
[5] Senckenberg Research Institute and Natural History Museum, Frankfurt am Main, Germany
[*] Authors to whom any correspondence should be addressed.

**E-mail:** norman.steinert@cicero.oslo.no and wunderling@c3s.uni-frankfurt.de

**Keywords:** permafrost carbon feedback, climate tipping, climate mitigation, overshoot, simple climate modeling

Supplementary material for this article is available online

## Abstract

Global warming leads to widespread permafrost thaw and subsequent emissions of carbon dioxide and methane, driving the permafrost carbon–climate feedback (PCF) which amplifies climate change. Many current-generation climate models omit this feedback, limiting projections of long-term temperature outcomes and associated Earth system tipping risks. Here, we investigate how this feedback affects the risk and timing of crossing tipping points in the Earth system by integrating permafrost carbon emissions into temperature projections for idealized stabilization and overshoot scenarios. In a conceptual network model of interacting climate tipping elements—including the Greenland and West Antarctic ice sheets, the Atlantic Meridional Overturning Circulation, and the Amazon rainforest, we find that PCF leads to additional warming that increases the probability of exceeding one or more tipping elements by up to 50% and can substantially accelerate the timing of tipping events by hundreds of years. The effect of PCF on tipping risk and acceleration is particularly evident in overshoot scenarios with lower peak temperatures below 2–3 °C or peak cumulative emissions of below 2000 PgC. Considering PCF, therefore, narrows the critical temperature space for overshoot pathways. Our results highlight that failing to account for PCF underestimates both climate risks and the urgency of mitigation, increasing the likelihood of tipping events across the Earth system.

## 1. Introduction

As global temperatures continue to rise, the risk of crossing climatic tipping points of critical Earth system elements such as the Greenland and West Antarctic ice sheets, the Atlantic Meridional Overturning Circulation (AMOC) or the Amazon rainforest increases [1, 2]. After crossing these tipping points, climatic systems and their associated ecosystems may undergo detrimental and irreversible changes, with potentially massive impacts on nature and society [1, 3]. Crucially, once tipping is initiated, self-reinforcing feedback mechanisms lock the climate system into ongoing change, thereby prolonging or amplifying impacts independently of future emission trajectories.

Among the most relevant climate feedbacks, the permafrost carbon–climate feedback (PCF) presents a significant threat to global climate stability [4, 5]. Permafrost soil, that is soils containing permanently frozen ground found in high-latitude regions, holds vast amounts of organic carbon, sequestered over millennia [4]. Due to Arctic amplification [6, 7], permafrost is thawing at an accelerating pace [8, 9], releasing significant quantities of carbon dioxide ($CO_2$) and methane ($CH_4$) in the process. The release of these greenhouse gases intensifies the greenhouse

effect, creating a potentially positive feedback which further warms the planet [4, 5].

Permafrost thaw interacts with climate tipping elements through a network of climate feedbacks that can both amplify and dampen warming, stabilize and destabilize ecosystems, and have cascading effects across the Earth system [10, 11]. The additional warming from permafrost carbon release, estimated at 21 (4–48; 5%–95% range) PgC/ °C in 2100 (Intergovernmental Panel on Climate Change's 6th assessment report; Box 5.1) [12], increases the likelihood of crossing tipping points across the Earth system, potentially leading to a domino effect of mutually reinforcing, and sometimes stabilizing, climate feedbacks. For example, enhanced warming from permafrost emissions can accelerate the melting of the Greenland Ice Sheet, contributing to sea level rise and disrupting ocean circulation patterns, such as the AMOC, leading to shifts in regional climates and rainfall patterns, which may further stress ecosystems like the Amazon rainforest [10]. High-latitude warming could also intensify boreal forest wildfires and sea ice loss, both of which reinforce the PCF through increased carbon release [13, 14] and albedo reduction [15, 16], respectively. As some processes like $CO_2$ fertilization and vegetation expansion may partly offset these effects, the strength of the PCF is heavily influenced by the capacity of natural carbon sinks. Ocean and land sinks help mitigate warming by absorbing $CO_2$, but their effectiveness is expected to decline under warming [17], with the land carbon sink already showing significant weakening trends over key Earth system biomes such as the Amazon rainforest [18–20]. This weakening reduces their ability to slow permafrost thaw and compensate for any additional carbon emissions from permafrost, thereby damping climate change less and highlighting the importance of how these sinks are represented in climate models [21].

The role of the PCF in the Earth system response to warming and its relation to tipping interactions is addressed in some studies [3, 5, 22–25] but remains underexplored, both from observational and modeling standpoints [10]. This knowledge gap limits a comprehensive understanding of how carbon emissions from permafrost thaw could amplify tipping risks. Here, we examine the potential effects of the PCF on both the risk and timing of crossing Earth system tipping points by integrating permafrost carbon emissions in climate change simulations of idealized stabilization and overshoot scenarios. By propagating temperature projections from the simple climate model FaIR [26, 27], with and without the PCF, to the tipping network model PyCascades [28]—a simplified model to quantify tipping risks in a coupled network of four core tipping elements, we assess PCF-induced global warming and its subsequent effect on tipping risks and timings.

## 2. Methods

### 2.1. Climate change emission pathways

We design a total of 73 emission scenarios to follow specific pathways of cumulative emissions (figure S1). For all scenarios, cumulative emissions ramp up over 200 years to nine levels of peak cumulative emissions ($cumE_{peak}$), ranging 1000 PgC to 3000 PgC in increments of 250 PgC (9 variants). The emission ramp-up follows a linear growth of emissions for 100 years and declines to zero in the next 100 years. Thereafter, emissions either stabilize at zero emissions (stabilization commitment scenarios; SC hereafter), or return to a cumulative emissions level of 1000 PgC following the same but now reversed cumulative emission curve (overshoot scenarios; OS hereafter) by assuming idealized carbon dioxide removal (CDR). For stabilization scenarios, combining $cumE_{peak}$ with subsequent zero emissions creates 9 variants. For overshoot scenarios, the 1000 PgC case is excluded (as it does not go beyond the cumulative emissions level of 1000 PgC), therefore giving 8 $cumE_{peak}$ variants. Also for overshoot scenarios, CDR is applied, varying its convergence time ($t_{conv}$) to return to 1000 PgC in the duration of 100 to 800 years in increments of 100 years, therefore giving another 8 $cumE_{conv}$ variants. Combining the variants for $cumE_{peak}$ and $t_{conv}$ creates 64 overshoot scenarios. All scenarios have converged their cumulative carbon emissions, at the latest, after 1000 years. These scenarios follow the notations of $SC^x$ and $OS^x_y$. Here, $x$ denotes the cumulative emission peak $cumE_{peak}$, which at the same time is the stabilization level in the stabilization scenarios, and $y$ denotes the convergence time $t_{conv}$ for the overshoot scenarios. The amount of CDR in the overshoot scenarios is therefore equal to $x - 1000$ PgC. This scenario framework allows us to explore a comprehensive space of cumulative emission levels and subsequent application of CDR.

### 2.2. FaIR simple climate model

The FaIR simple climate model (version 1.6.4) [26, 27] is designed to simulate the global climate system's response to greenhouse gas emissions and short-lived climate forcers. FaIR models atmospheric carbon dioxide and other greenhouse gases with an impulse response function. The model includes components for radiative forcing, carbon cycle feedbacks, and simple climate response dynamics, making it suitable for analyzing temperature responses under various emission scenarios, including overshoot and mitigation pathways. Additionally, FaIR is computationally efficient, which supports its use in probabilistic analyses and comparisons of long-term climate stabilization pathways. FaIR is calibrated to produce plausible temperature responses for a range of emissions scenarios matching broad climate behavior of complex Earth system models and represents their climate response

uncertainties [26, 27]. This calibration is not a strict fit to observational datasets in a statistical sense but is consistent with the original FaIR formulation and legacy tuning from earlier model versions [26, 27], which makes it a suitable tool for the implementation of the PCF.

### 2.3. PyCascades tipping network model

PyCascades is a network model operating on a probabilistic basis using simplified mathematical representations (equation (1)) of individual tipping elements and interactions between them [28]. These interactions can be both positive (amplifying) and negative (damping), which allows exploration of how tipping dynamics might unfold under different climate scenarios. PyCascades is computationally efficient, making it suitable for testing a wide range of climate scenarios, particularly in terms of how specific climate thresholds, mitigation strategies, or global temperature changes affect the risk of (multiple) tipping events [29, 30]. In this study, we use PyCascades to assess the tipping risk and emerging cascading effects among four core climate tipping elements: the Greenland ice sheet (GIS), the AMOC, the West Antarctic ice sheet (WAIS), and the Amazon rainforest (AMAZ). In PyCascades, tipping elements are represented by differential equations of the form:

$$\frac{\mathrm{d}x_i}{\mathrm{d}t} = \left[ x_i - x_i^3 + \sqrt{\frac{4}{27}} \times \frac{\Delta GMT(t)}{T_{\mathrm{crit},i}} + \mathrm{d} \times \sum_{j \neq i} \frac{s_{ij}}{10} \left(x_j + 1\right) \right] \frac{1}{\tau_i}. \quad (1)$$

Here, $x_i$ represents the state of each tipping element. The differential equation has two stable states: a baseline around $x_i \approx -1$ (initial condition) and a transitioned state near $x_i \approx +1$. The increase of the global mean surface temperature change beyond pre-industrial levels is denoted $\Delta GMT(t)$, and $T_{\mathrm{crit},i}$ marks the critical temperature for each tipping element [1]. Link strength values $s_{ij}$ represent interaction mechanisms. While these values are quantified [28, 31], the absolute impact of each interaction is uncertain. To account for this uncertainty, PyCascades introduces the interaction-strength parameter $d$, which we vary here between 0 and 0.5 in steps of 0.1. A value of $d = 0$ implies no interaction between the tipping elements, while $d = 0.5$ suggests that interactions are roughly half as influential as each element's individual dynamics [28, 31]. This approach allows us to explore a broad range of potential interactions among the tipping elements. The timescale parameter $\tau_i$ reflects the transition time of each tipping element. The temperature tipping point thresholds and response timescales are set to the central (upper-to-lower limit) estimates, respectively [1]: 1.5 (0.8–3.0) °C and 10 000 (1000–15 000) years for GIS, 4.0 (1.4–8.0) °C and 50 (15–300) years for AMOC, 1.5 (1.0–3.0) °C and 2000 (500–13 000) years for WAIS, and 3.5 (2.0–6.0) °C and 100 (50–200) years for AMAZ. To represent uncertainty in these estimates, we use a sampling of these parameters (see section 2.5).

### 2.4. Implementation of the PCF

The analysis of the PCF impacts on Earth system tipping requires different sets of climate simulations to separate its effects. For this study, we implement the permafrost carbon feedback in FaIR using the simple permafrost carbon response model PerCX (equation (2)) [32, 33]. This gives us a modified version of FaIR that incorporates an idealized representation of the PCF (FaIR-PerCX or 'PCF' case hereafter) that can be compared to the standard version of FaIR without the PCF ('base' case hereafter). Here, the combined FaIR-PerCX is not recalibrated because the PCF effect during the historical period is small and to ensure a cleaner comparison between the base and PCF cases. PerCX emulates the permafrost carbon response to climate determined by the sum of the $CO_2$ and $CH_4$ responses:

$$\Delta C_{\mathrm{PF}}(t) = \left(A_{\mathrm{CO_2}} + A_{\mathrm{CH_4}}\right) \cdot \int_0^t \Delta T(t') \cdot \frac{C_{\mathrm{p}}(t')}{C_{\mathrm{p}}(0)} \cdot \mathrm{e}^{\frac{-(t-t')}{\tau}} \, \mathrm{d}t', \quad (2)$$

with $\Delta T$ denoting the past temperature exposure, $C_{\mathrm{p}}(0)$ denoting the initial carbon pool of 1400 PgC [4, 34] at time $t = 0$ and $C_{\mathrm{p}}(t)$ denoting the time-evolving combined leftover $CO_2$ and $CH_4$ permafrost carbon pool at time $t$. Both $CO_2$ and $CH_4$ emissions from permafrost are determined by an exponential decay function that accounts for temperature history, and are converted to units of carbon. $A_{\mathrm{CO_2}}$ and $A_{\mathrm{CH_4}}$ are coefficients for the amplitude of $CO_2$ and $CH_4$ emissions that are released on a combined response timescale $\tau$. All parameters are derived by calibrating PerCX against PCF estimates given in the Intergovernmental Panel on Climate Change's (IPCC) 6th assessment report [32], which here yields 776 parameter combinations. While the calibration of the original version of PerCX v1.0.1 uses a fixed $CO_2$–$CH_4$ ratio of 6/1 [32], here we use PerCX v1.0.2, which adjusts the calibration process to incorporate a probabilistic sampling of the $CO_2$-$CH_4$ ratio ranging between 5/1 and 100/1 to account for a wide range of possible variety in microbial community composition and associated microbial metabolisms [35, 36]. Considering a variable $CO_2$-$CH_4$ ratio makes PerCX v1.0.2 overall slightly less sensitive to warming. PerCX assumes the carbon release timescales for $CO_2$ and $CH_4$ to be identical. These emissions are then fed individually into FaIR, which internally handles their differences in lifetime and associated effective forcing. In the comparison with other models, PerCX produces a slightly larger permafrost carbon response than UVic [37, 38] and PAGE-ICE [39],

largely because it is calibrated to the broader CMIP range rather than a single model and has a comparatively larger initial carbon pool [39, 40], though it still overlaps with these models at the lower end of that range [32]. Due to this calibration, PerCX represents a suitable estimate of permafrost responses arising from uncertainty in CMIP land surface models.

### 2.5. Modeling chain and uncertainty propagation

Running the modeling framework (with and without PCF) follows several steps. Prescribed emissions data follow the trajectories corresponding to our stabilization and overshoot scenarios. From these emissions, FaIR creates global mean temperature projections, which are subsequently propagated to PyCascades. All emissions of non-$CO_2$ species (the PCF-related methane emissions not accounted for) are kept constant at pre-industrial levels throughout the entire simulations.

In order to capture tipping dynamics of the ice sheets in PyCascades, all simulations have a total duration of 10 000 years. However, the temperature timeseries from FaIR and FaIR-PerCX are only simulated for 1000 years and held constant afterwards. In addition to computational efficiency (in particular for the PCF case), the first 1000 years capture the transient climate response and feedback-driven warming relevant for forcing ice sheets. Further, because PerCX is calibrated to 21$^{st}$ century estimates, extrapolations beyond a millennium could result in biased projections. Although temperatures are likely to slightly decrease (in relative terms) on millennial timescales because of long-term land and ocean carbon uptake that reduces atmospheric $CO_2$ concentration, keeping temperature constant beyond year 1000, equivalent to assuming the climate system has reached a quasi-steady state, creates a relatively small bias and maintains the PCF-induced temperature offset most relevant for this analysis.

Throughout the entire modeling chain, we simulate 1000 ensemble members. The parameters of each model component in this chain are sampled from their individual parameter pools and therefore create a unique combination of parameters across all components for each ensemble member. First, FaIR's sampling is based on 2237 parameter combinations [41–43], from which we select 1000 with a uniform random direct sampling (figure S2). Second, this sampling approach is applied to the PerCX parameters. Here, the selection of 1000 members increases the original ensemble size of 776 parameter combinations from PerCX' calibration (figure S3). For the simulations with FaIR-PerCX, we ensure that the parameters sampled are identical between FaIR and FaIR-PerCX. Third, we sample PyCascades following the same approach, which includes the sampling of tipping point warming thresholds and timescales for all four tipping elements. Since the literature typically only provides the central estimate as well as lower and upper bounds, we create a prior skew-normal distribution of 10 000 values (figure S4) with its median representing the central estimate and upper-to-lower values confined by the boundary estimates (see section 2.3). Then, for the posterior, again 1000 members are directly resampled from the prior distribution. The PyCascades sampling also includes parameter choices from interaction strength and direction of interaction between tipping elements, also sampled uniform-randomly (figure S5). Figures S2–S4 illustrate that resampling to 1000 members still retains the general features of the prior distribution in the posterior distribution.

The 1000-member ensemble of the modeling chain is run for all 73 scenarios, resulting in 73 000 simulations. First, this is done without the PCF (FaIR $\rightarrow$ PyCascades), generating the baseline temperature timeseries. Then the runs are repeated including the PCF (FaIR-PerCX $\rightarrow$ PyCascades) to yield results that can be compared to the simulations without PCF to isolate its effect on tipping risk and timing.

## 3. Results and discussion

### 3.1. Permafrost feedback on temperature

Figure 1(a) shows example trajectories for a stabilization at 1000 PgC ($SC^{1000}$) and 1250 PgC ($SC^{1250}$), as well as overshoot of 250 PgC with a cumulative emissions peak at 1250 PgC and a convergence time back to 1000 PgC of 100 years ($OS^{1250}_{100}$), illustrating the smallest and shortest overshoot in our scenario ensemble. The global mean temperature projections of these scenarios (figure 1(a)) run by FaIR ('base') and FaIR-PerCX ('PCF') illustrate the effect of PCF on temperature (figure 1(b)).

For the median base temperatures, $SC^{1000}$ scenario ramps up to, and stabilizes at, around 1.4 °C, while the overshoot scenario $OS^{1250}_{100}$ peaks at around 1.75 °C (also see figure S6) and returns to its $SC^{1000}$ reference temperature with a small temporary temperature increase of less than 0.1 °C after emissions cease, within 1000 years. Such temporary temperature increase after emissions cease can also be seen in the $SC^{1250}$ scenario, which approximately returns to 1.75 °C after 1000 years. From here, temperatures are set constant over an additional 9000 years.

When PCF is included, median temperature outcomes are substantially higher. $SC^{1250}$ with PCF peaks about 0.2 °C higher than without, and both $SC^{1000}$ and $OS^{1250}_{100}$ follow a continuous increase in temperatures after zero emissions. Their median temperature reached after 1000 years is 2.2 °C, about 0.8 °C higher than without PCF. There is a small but visible difference between the two, which illustrates the impact of the overshoot on the PCF contribution. In FaIR-PerCX, cumulative temperatures are higher for the overshoot than for the non-overshoot, which increases permafrost carbon emissions accordingly

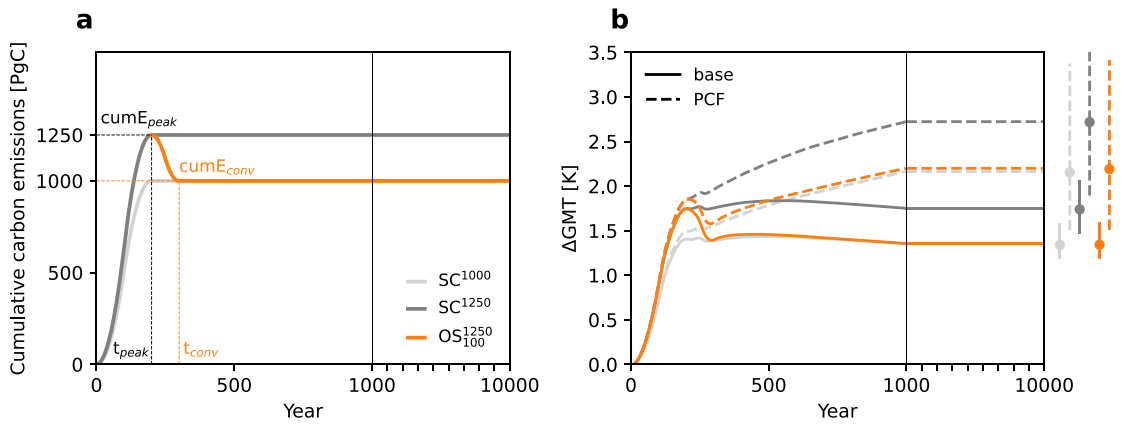


**Figure 1.** Permafrost carbon–climate feedback on temperature: (a) Cumulative carbon emissions for a subset of scenarios illustrating examples of stabilization (SC) and overshoot (OS) emission pathways used to generate temperature in FaIR. (b) Temperature estimates from FaIR based on the scenarios in panel (a) for both 'base' (without PCF) and 'PCF' (with PCF) model configurations. Uncertainty ranges for the 5th to 95th percentiles from the probabilistic distribution of FaIR (effectively representing climate sensitivity and uncertainties in the permafrost carbon-climate feedback) are shown as whiskers on the right.

and results in a slightly higher forcing, which in turn generates slightly higher temperatures for $OS^{1250}_{100}$ than for $SC^{1000}$. It is also evident that the additional forcing from permafrost carbon emissions counteracts the CDR, which would now have to be larger to equalize the resulting additional warming. Hence, $SC^{1250}$ shows substantially higher temperatures of up to 2.75 °C after 1000 years for PCF, an increase of 1.0 °C, with a slightly growing gap until the two simulations stabilize at 1000 PgC until year 10 000. The 5th–95th percentile range of temperature for the simulations without PCF is relatively small at about 0.4 °C (figure 1(b), whiskers). This range increases substantially for the simulations with PCF. The result is an uncertainty range of up to 2.0 °C for the three example scenarios shown here. Similar temperature trajectories are simulated for the rest of the scenario ensemble.

### 3.2. Amplified tipping risks due to PCF

Running the FaIR-PyCascades modeling pipeline for all 9 stabilization and 64 overshoot emissions scenarios generates a variation of responses for the four tipping elements GIS, AMOC, WAIS and AMAZ—here shown for all ensemble members without PCF (figures 2(a)–(d)). A system state of $\sim -1$ describes an (initial) stable state, which can transition to an alternative stable state of $\sim +1$. After the initial forcing ramp-up, all systems initially respond with a shift to a more unstable state. Depending on the system's response timescales and their interactions, as well as the temperature trajectory they are exposed to, they subsequently either transition to the alternative stable state, or stabilize again.

For GIS, most stabilization scenarios (black) lead to tipping, primarily depending on whether stabilization temperatures exceed its critical threshold. In contrast, fewer overshoot scenarios result in tipping, as temporary overshoots followed by cooling can reduce GIS's tipping risk due to its slow response time, allowing it to resist short-term warming perturbations [29, 44, 45]. GIS can remain in transitional states for long periods, unlike AMOC and AMAZ, which switch states more rapidly. AMOC does not stay in transition for long and may start tipping over a wide range of years. This could indicate that AMOC tipping is often driven by other systems' (e.g. GIS) state transitions, which is consistent with a proposed AMOC slowdown from North Atlantic freshwater influx from GIS melt [46, 47]. AMAZ behaves similarly, though more scenarios keep it in its initial state. Its transitions also span the simulation period and suggest interactions with GIS and AMOC in a cascading sequence [46]. WAIS exhibits much faster tipping behaviour than GIS, often within the first millennium. Only overshoot scenarios with the lowest peaks and fastest recovery can avoid WAIS tipping.

The effects of PCF increase tipping risk across all four elements (figures 2(e)–(h)). Scatter points in the lower left and upper right corners mean that non-PCF states (base) and PCF states (PCF) agree, i.e. there is no state difference between the two cases, regardless of whether it is in the initial or the alternative stable state. Conversely, scatter points in the upper left corner indicate a tipped state in the PCF case, whereas the base case is still in its initial state, and vice versa for the lower right corner. Scenarios with PCF (transition along $y$-axis) often show earlier tipping than their non-PCF counterparts (transition along $x$-axis). In such cases, PCF system transitions occur sooner in the simulation, which is why there are a lot of scatter points in the upper left corner. This is especially evident for ice sheets, where slow transition dynamics cause PCF and non-PCF states to diverge during tipping. These effects are consistent across both stabilization and overshoot pathways and are determined by the forcing pressure from the cumulative emission pathways.

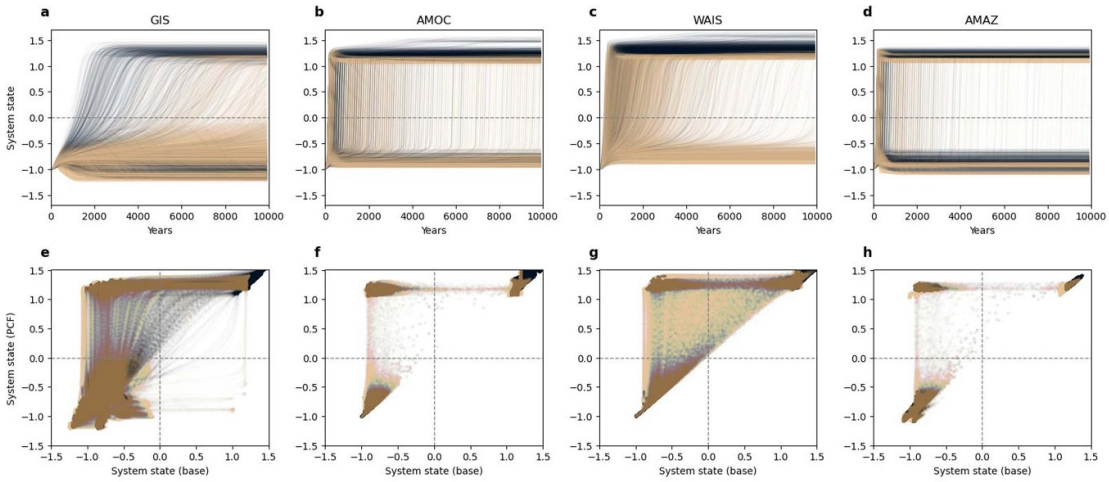


**Figure 2.** State evolution of tipping elements under stabilization and overshoot scenarios: (a)–(d) State transitions for the four tipping elements in PyCascades: Greenland Ice Sheet (GIS), West Antarctic Ice Sheet (WAIS), Atlantic Meridional Overturning Circulation (AMOC), and the Amazon rainforest (AMAZ), for all 1000 ensemble members for the case without PCF ('base'), times 73 scenario pathways. The scenarios are split into 9 stabilization (black) and 64 overshoot (orange) pathways. (e)–(h) State comparison scatterplots with points at each timestep of all scenarios in panels (a)–(d) between 'base' (without PCF) and 'PCF' (with PCF) cases. Points in the lower left and upper right corners mean equal states between the two case; points in the upper left corner means that PCF case tipping happens before the base case tipping.

Tipping risk generally increases with peak temperature, both in stabilization and overshoot scenarios (figures 3(a)–(d)), consistent with previous studies [29, 30, 45]. Tipping risk is assessed here as the occurrence of at least one transition above a state threshold of +0.577 (crossing the mathematically exact stable state of $\frac{1}{\sqrt{3}}$ [48]), regardless of whether the system remains in the alternative stable state or not for the remainder of the simulation. This definition of tipping risk is useful because tipping of any of the four tipping elements would cause significant harm to society, be it due to strong sea-level rise from the ice sheets, interruption of the AMOC or dieback of the Amazon rainforest [49]. Stabilization commitment scenarios increase tipping risk relatively linearly with peak temperature because of their stepwise increase in cumulative temperature exposure (figure S7). PCF's effect on tipping risk follows the same relationship, but leads to higher peak temperatures and temperature exposure over time. The risk increase from overshoot is steeper for AMOC, WAIS and AMAZ than for GIS. Overall, this indicates that any overshoot can increase the tipping risk compared to its counterfactual low stabilization scenario, but also that it prevents higher tipping risk compared to a higher stabilization scenario. For AMOC and WAIS, PCF yields an increased tipping risk of around 40%, which is particularly evident for low overshoots with peak temperatures below 3 °C. For GIS (+30%) and AMAZ (+20%), it is more homogeneous across peak temperature levels. While cumulative temperature exposure can be similar between overshoots (figure S7), the peak temperatures over shorter timescales play a role in modulating tipping risks and indicate a strong path dependence of AMOC and AMAZ. For example, a large overshoot with a short convergence time might have the same cumulative temperature exposure as a lower stabilization scenario. However, the high peak temperature of the overshoot may cause a temporary crossing of the critical warming threshold for AMOC or AMAZ (both of which have relatively high thresholds of 3.5 °C and 4 °C), which can lead to tipping owing to their fast response timescales.

The influence of the PCF in increasing tipping risks is evident in all tipping elements (figure 3(e)–(h)). Stabilization scenarios show larger tipping risks than associated overshoot scenarios, owing to their stabilization at high temperature levels. Nonetheless, tipping risk under overshoot can be much enhanced by PCF. For example for GIS, many overshoot scenarios have a base tipping risk below 10%, while it is at around 40% for PCF simulations (also see figure S7). This difference decreases the larger the base tipping risk becomes, but has large implications for the average tipping risk increase from PCF. AMOC and WAIS both already show comparatively high risks of tipping without PCF across scenarios. Regardless, PCF can substantially increase tipping risks with as much as 40% for low overshoot scenarios. This also means that, with PCF, tipping risk is above 90% for WAIS and above 70% for AMOC for overshoot peaks of below 2 °C, equivalent to below 1500 PgC (figure S6).

Isolating the effects of PCF for the overshoot, grouping them by overshoot peak emissions, reveals different patterns for the different tipping elements (figure 3(i)). GIS tipping risks are around 35%, and remain high for all levels of peak overshoot because of GIS's combination of a low critical warming threshold and its slow response timescale. Increased

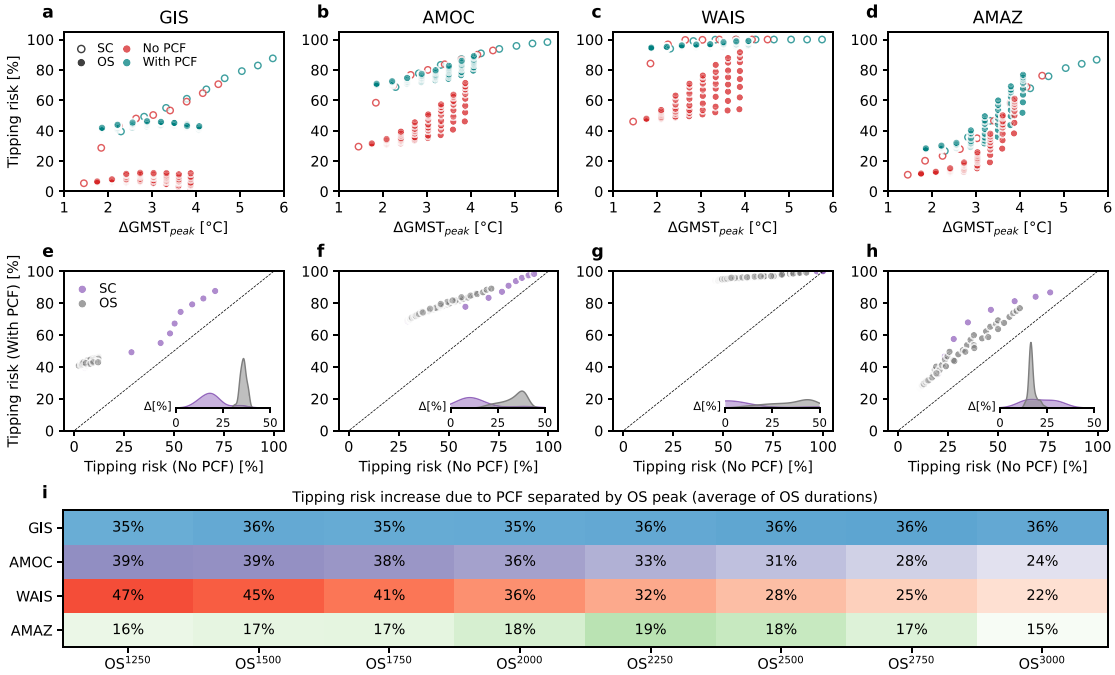


**Figure 3.** Effects of PCF on tipping risks: (a)–(d) Absolute tipping risks for the four investigated tipping elements with respect to stabilization (SC, hollow points) and overshoot (OS, filled points) peak temperature for 'base' (without PCF; red) and 'PCF' (with PCF; teal) cases. (e)–(h) Tipping risk comparison between 'base' (*x*-axis) and 'PCF' (*y*-axis) cases, i.e. how much the tipping risk increases due to PCF, for SC (purple) and OS (gray) scenarios. (i) Heatmaps of increased tipping risk due to PCF separated by overshoot peak emissions (averaged over 8 overshoot durations). The numbers represent the additional risk contribution from PCF for each of the overshoot scenarios, and the heatmap color scales are normalized per element to illustrate their changes with increasing emissions overshoot.

warming exposure from PCF in each overshoot scenario group can therefore affect its tipping dynamics homogeneously across scenarios. For AMOC and WAIS, increased tipping risks from PCF mainly affect overshoots with lower peak emissions, with tipping risks of 39%–47%. With higher emission peaks, PCF-induced increases in tipping risks change from 39% to 24% for AMOC, and from 47% to 22% for WAIS. This means that both AMOC and WAIS have much enhanced tipping risks from PCF for small overshoots (figure S7) because PCF's effect is largest if base temperatures are close to the tipping point and only exceed it with the PCF temperature contribution. In contrast, in higher overshoots, more simulation ensemble members are tipped already in the 'base' case, for which the additional warming of the PCF does not add additional risk of tipping. This means that climate tipping risks could be underestimated by not considering the PCF if global warming would approach a critical temperature threshold of a given tipping element. The results mirror the behavior seen in panels (e)–(f). AMAZ is the only element for which tipping risk slightly increases with larger overshoot. Its risk increase due to PCF peaks at 29%. Overshoots, peaking around 2000–2500 PgC of cumulative emissions, generate temperatures closest to the critical warming threshold of AMAZ. This means that in these cases the additional warming from PCF causes AMAZ to tip, whereas in the base case, temperatures would stay slightly below this threshold. Lower and higher overshoots, instead, are more likely to have a stable or tipped state in both base and PCF simulations, which slightly decreases the impact of the PCF, respectively.

### 3.3. Critical temperature spaces for tipping risks

Based on all tipping timeseries, we investigate the tipping risks' dependence on the overshoot peak temperature and the convergence time (time until cumulative emissions have reached 1000 PgC after the overshoot). Without the influence of the PCF, we find that tipping risks are generally high for WAIS and AMOC (figures 4(b) and (c)). They show tipping risks of 50% with an overshoot peak temperature of 1.8–2.8 °C for WAIS and 3.0–4.0 °C for AMOC depending on the overshoot duration. In the case of WAIS, the final stabilization temperatures lie above its tipping point in many cases. AMAZ shows a tipping risk lower than 20% for overshoot peak temperatures below 3.0 °C regardless of the overshoot duration (figure 4(d)). However, higher overshoots (with peak temperature close to its tipping point) show a strong increase of tipping risks, owing to its relatively fast response timescale. Consistent with figures 2 and 3, overshoot keeps GIS tipping risks relatively low, i.e. below 15% (figure 4(a)). These results are comparable with other studies [29, 30].

We find that the PCF considerably narrows the risk zones to lower overshoot peak temperature and duration for all tipping elements

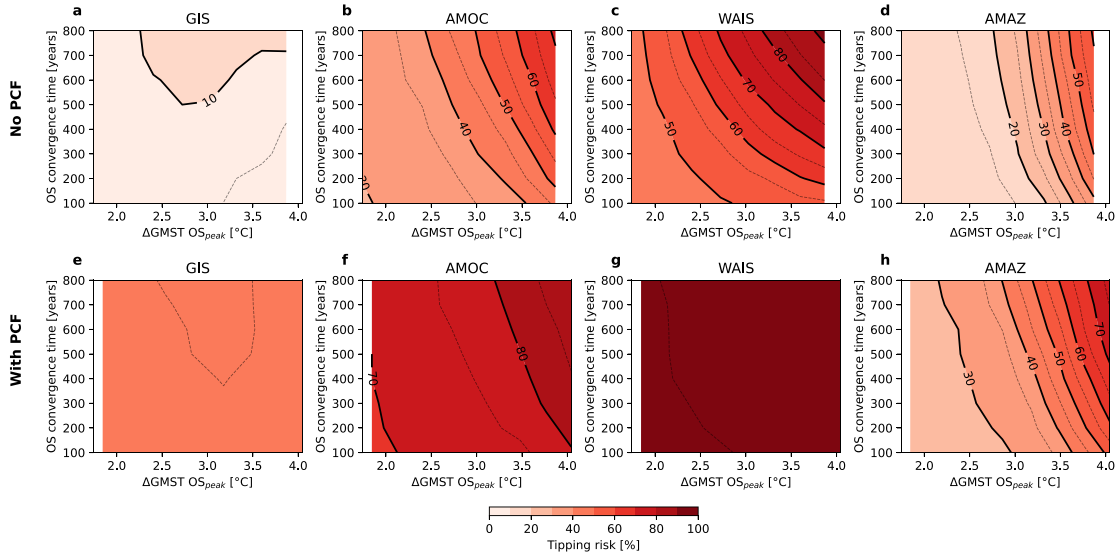


**Figure 4.** Critical temperature spaces for tipping risks under overshoot: (a)–(d) Tipping risks (color scale) depending on the overshoot peak temperature ($OS_{peak}$) and overshoot convergence time until cumulative emissions have reached 1000 PgC after the overshoot. (e)–(h) Same as panels (a)–(d) but for the simulations including the PCF. Note that the respective PCF and non-PCF panels span different temperature range due to the effect or absence of the PCF contribution to temperature.

(figures 4(e) and (f)). All tipping risk increases are in the range of 20%–40% for specific overshoot peak temperatures and durations (also see figure S7). This increases the tipping risk to about 40% for GIS because of its slow response timescale. AMOC's tipping risk increases to at least 70% even with an overshoot peak temperature of below 2 °C. Similarly, AMAZ's risk zone substantially reduces to lower overshoot peak temperatures. More importantly, AMAZ's sensitivity to overshoot duration also increases when including PCF. For example, a 50% chance of AMAZ tipping is reduced by about 1 °C (from approximately 3.2 °C to 2.2 °C) for long overshoots with PCF. While WAIS already has high risks of tipping above 45% without PCF, considering PCF brings its tipping risk to 94%–99% even for the shortest 100-year overshoots below 2 °C.

### 3.4. Tipping acceleration due to PCF

Besides PCF's effect on tipping risks, we also quantify its impact on the timing of simulated tipping events. Here we define the tipping timing as the first time a system state crosses the threshold for the alternative stable (system state 0.577). Tipping timing follows a reverse relationship with peak temperature across all tipping elements (figures 5(a)–(d)) and is earlier with increasing peak temperature. There is a high acceleration of this timing under low stabilization and overshoot scenarios, concurring with lower cumulative warming exposure (figure S7). GIS's tipping times range from 8000 years in scenarios that just tip before the end of the simulation to as early as 2000 years. In contrast, AMOC, WAIS, and AMAZ can all have a range of ensemble-mean tipping times between a few decades and up to 4000 years, which quickly reduces in higher peak warming scenarios. Although AMOC and AMAZ are faster tipping elements than WAIS, WAIS often has an earlier state transition onset because it has a low temperature tipping threshold. While AMOC and AMAZ state transition happens faster, their tipping onset may happen later in the simulations, depending on the scenario. Across all scenarios and ensemble members, WAIS's tipping times are therefore the fastest.

The timing of tipping due to PCF can be faster on the order of decades to thousands of years (figures 5(e)–(h)). GIS tipping acceleration can be as high as 4000 years. However, there is a clear separation between stabilization and overshoot scenarios. For AMOC, WAIS and AMAZ, the responses are more diverse than for GIS. Their tipping acceleration can range from no acceleration to up to 4000 years, with no substantial difference between stabilization and overshoot scenarios. Matching the results of tipping risks, there is a minority of cases for AMOC and AMAZ where PCF delays the tipping timing, but only by a maximum of a few centuries. For the high-warming stabilization scenarios, tipping across all tipping elements often occurs regardless of PCF. Instead, PCF in overshoot scenarios tends to cause tipping accelerations of 3000–4000 years. That is because in many overshoot scenarios without PCF, early tipping can be prevented by the lower cumulative warming exposure. However, the PCF substantially increases this cumulative warming exposure, which leads to earlier tipping.

The tipping acceleration due to PCF is highest for the low-to-mid overshoots (1250–2000 PgC of peak cumulative emissions; about 1.5–2.5 °C peak warming; figure S6) across all tipping elements (figure 5(i)). Higher overshoots generally show much lower acceleration of tipping timing for

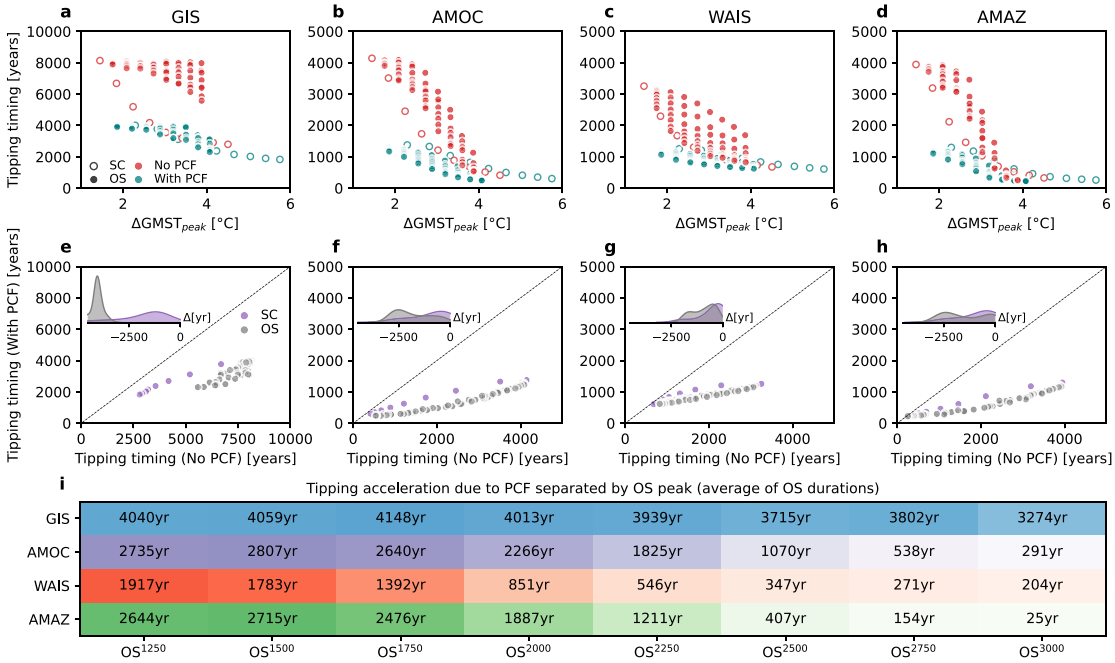


**Figure 5.** Effects of PCF on the timing of tipping events: (a)–(d) Tipping timing for the four investigated tipping elements with respect to (stabilization and overshoot). (e)–(h) Tipping timing comparison between between 'base' (without PCF; *x*-axis) and 'PCF' (with PCF; *y*-axis) cases, i.e. how much the tipping accelerates due to PCF. (i) Heatmaps of tipping acceleration due to PCF separated by overshoot peak emissions (averaged over 8 overshoot durations). The numbers represent the distribution-weighted average tipping acceleration due to PCF (see figure S8) for each of the overshoot scenarios, and the heatmap color scales are normalized per element. Note the difference in *y*-axis range between the panels.

AMOC, WAIS, and AMAZ, decreasing from multiple millennia to centuries, and even decades in the case of AMAZ. This is, again, due to the faster tipping in scenarios with a high warming exposure, where tipping happens regardless of the PCF. The exception is GIS, where the influence of PCF is seen across the full range of overshoots, matching the behavior of tipping risks.

## 4. Conclusions

The permafrost carbon–climate feedback (PCF) plays an important role in amplifying Earth system tipping risks. We find that assessed ranges of PCF contribute to increased global warming, which in turn elevate the likelihood of tipping critical Earth system components. This effect is particularly strong for WAIS and AMOC, where including PCF raises tipping probabilities by up to 50% and leads to earlier tipping. GIS tipping risk also increases, though less dramatically, likely due to its slow response timescale and stabilizing interactions with AMOC. Notably, including the PCF can cause tipping even in low peak temperature overshoot scenarios that otherwise would remain below critical thresholds. For example, with PCF, tipping risk is above 90% for WAIS and above 70% for AMOC for overshoot peaks of below 2 °C, while it increases to around 40% for GIS and AMAZ below 3 °C. Equally, tipping acceleration due to PCF is highest for the low-end overshoots (1250–2000 PgC of peak cumulative emissions or about 1.5–2.5 °C peak warming).

Furthermore, it is evident that the effect of the PCF is highest when scenario pathways bring temperatures close to the tipping thresholds of a specific system, for which the additional warming from the PCF results in a tipping of the otherwise stable system. For faster tipping elements, such as the AMOC and AMAZ, this means that peak temperatures substantially influence the tipping behaviors. Conversely, for slower systems, such as GIS, it is rather the cumulative warming exposure that leads to a slow transition out of its stable state. The PCF also accelerates the timing of tipping, reducing the safe overshoot temperature range and making climate stabilization efforts more challenging. This acceleration is pronounced for systems with both inherently slow and fast tipping dynamics, where PCF can advance tipping timing by thousands of years, predominantly found in lower-end overshoot scenarios ranging 1250–2000 PgC of peak cumulative emissions.

The presence of the PCF also redefines the climatic risk space for tipping by shifting the boundaries of temperature overshoot and duration within which tipping can be avoided. With PCF, the critical zones for tipping risks of 50% substantially shift toward lower peak temperatures (below 2 °C for GIS, AMOC and WAIS; below 3.5 °C for AMAZ) and shorter overshoot durations (as little as 100 years for GIS, AMOC, WAIS). These shifts underscore the

fact that tipping elements are more vulnerable than previously assumed when considering the effects of PCF, and consequently that climate targets which permit temporary overshoots may lead to irreversible changes when PCF is included.

This is a conceptual risk study. Both the conceptual scenario design and the treatment of temperature evolution over 10 000 years are idealized and in addition ignore non-$CO_2$ species contributions and anthropogenic disturbances, so the quantities derived here are associated with uncertainties. However, despite the inclusion of only a subset of tipping elements simulated in PyCascades with simplified threshold behavior and interactions, it can actually represent these interactions, opposed to either Earth system models that often do not show tipping behavior or conceptual tipping models that only capture the dynamics of a single tipping element. We further note that the implementation of the PCF used here is rather simple. Although calibrated against estimates from complex Earth system models and their uncertainties, PerCX does not explicitly resolve the processes that enhance natural carbon sinks that could weaken the effect of the PCF, such as $CO_2$ fertilization, vegetation expansion, nitrogen fertilization and formation of new permafrost carbon at high latitudes. Explicitly accounting for these effects, in addition to yet undiscovered and unrepresented feedbacks on permafrost carbon loss itself, may modify PCF's impact on the estimate of increased tipping risks and acceleration provided here. These caveats present themselves as research priorities that should be addressed in future research.

Our results support a unified interpretation in which permafrost carbon feedback acts as a missing Earth system feedback in conventional carbon budget-based climate-policy metrics such as the Transient Climate Response to cumulative carbon Emissions (TCRE). Here, carbon released from permafrost in addition to anthropogenic emissions can be interpreted as a scaling factor for effective TCRE since total cumulative carbon driving warming is higher than accounted for in standard budgets estimates [32, 50, 51]. A more complete representation of permafrost thaw processes such as abrupt thaw, wildfire disturbances, and post-fire dynamics can therefore lead to an overestimation, and therefore tightening, of remaining carbon budgets consistent with temperature targets and may even introduce potential state-dependency [52]. In risk terms, it implies that the probability and timing of climate tipping events are underestimated. This reinforces the conclusion that pathways toward lower temperature targets become more attractive when Earth system feedbacks such as PCF are included, as they simultaneously reduce expected damages [39] and limit exposure to high-impact, potentially irreversible tipping dynamics.

Overall, these results reveal that the permafrost PCF could not only alter the probability of crossing tipping points but can also bring forward the timeline for potentially irreversible changes, reducing the window for effective climate mitigation. They underscore the necessity of including PCF in complex climate models, where it is often missing [50, 51]. Hence, current climate policies and emission pathways may underestimate the risks associated with permafrost thaw, necessitating more aggressive emission reductions and carbon removal strategies to mitigate these additional feedback-driven warming effects. An inclusion of the PCF in climate risk assessments is therefore essential for a more accurate estimation of safe emission thresholds and for designing effective climate policies.

## Acknowledgments

This work has been supported by the Research Council of Norway through the research project TRIFECTA (Grant no. 334811).

## Data availability statement

The data and the code supporting the findings of this study are openly available from the following URL/DOI: https://doi.org/10.6084/m9.figshare.31376533 [53].

Supplementary data 1 available at https://doi.org/10.1088/1748-9326/ae7586/data1.

## Conflict of interest

The authors declare no competing financial interests.

## Author contributions

Norman J Steinert 0000-0002-2154-5857
Conceptualization (lead), Data curation (lead), Formal analysis (lead), Investigation (lead), Methodology (lead), Software (lead), Visualization (lead), Writing – original draft (lead), Writing – review & editing (lead)

Gregory Munday 0000-0003-4750-9923
Conceptualization (supporting), Data curation (supporting), Formal analysis (supporting), Software (supporting), Visualization (supporting), Writing – review & editing (supporting)

Marit Sandstad 0009-0007-2329-694X
Conceptualization (supporting), Methodology (supporting), Writing – review & editing (supporting)

Benjamin M Sanderson 0000-0001-8635-4624
Conceptualization (supporting), Methodology (supporting), Writing – review & editing (supporting)

Nico Wunderling
Conceptualization (supporting), Methodology (supporting), Writing – review & editing (supporting)

## References

[1] McKay D I A, Staal A, Abrams J F, Winkelmann R, Sakschewski B, Loriani S, Fetzer I, Cornell S E, Rockström J and Lenton T M 2022 Exceeding 1.5C global warming could trigger multiple climate tipping points *Science* **377** eabn7950
[2] Lenton T M, Held H, Kriegler E, Hall J W, Lucht W, Rahmstorf S and Schellnhuber H J 2008 Tipping elements in the Earth's climate system *Proc. Natl Acad. Sci. USA* **105** 1786–93
[3] Winkelmann R *et al* 2025 The tipping points modelling intercomparison project (TIPMIP): assessing tipping point risks in the Earth system *Egusphere* pp 1–52
[4] Schuur E A G *et al* 2022 Permafrost and climate change: carbon cycle feedbacks from the warming arctic *Annu. Rev. Environ. Resour.* **47** 343–71
[5] Nitzbon J *et al* 2024 No respite from permafrost-thaw impacts in the absence of a global tipping point *Nat. Clim. Change* **14** 573–85
[6] Rantanen M, Karpechko A Y, Lipponen A, Nordling K, Hyvärinen O, Ruosteenoja K, Vihma T and Laaksonen A 2022 The Arctic has warmed nearly four times faster than the globe since 1979 *Commun. Earth Environ.* **3** 168
[7] Stroeve J C, Notz D, Dawson J, Schuur E A G, Dahl-Jensen D and Giesse C 2025 Disappearing landscapes: the arctic at +2.7C global warming *Science* **387** 616–21
[8] Biskaborn B K *et al* 2019 Permafrost is warming at a global scale *Nat. Commun.* **10** 264
[9] Turetsky M R *et al* 2019 Permafrost collapse is accelerating carbon release *Nature* **569** 32–34
[10] Wunderling N *et al* 2024 Climate tipping point interactions and cascades: a review *Earth Syst. Dynam.* **15** 41–74
[11] Ripple W J, Wolf C, Lenton T M, Gregg J W, Natali S M, Duffy P B, Rockström J and Schellnhuber H J 2023 Many risky feedback loops amplify the need for climate action *One Earth* **6** 86–91
[12] Canadell J G *et al* 2023 Global Carbon and Other Biogeochemical Cycles and Feedbacks *Climate Change 2021 – The Physical Science Basis* (Cambridge University Press) pp 673–816
[13] Zhu X, Jia G and Xu X 2024 Accelerated rise in wildfire carbon emissions from Arctic continuous permafrost *Sci. Bull. (Beijing)* **69** 2430–8
[14] McCarty J L *et al* 2021 Reviews and syntheses: Arctic fire regimes and emissions in the 21st century *Biogeosciences* **18** 5053–83
[15] Duspayev A, Flanner M G and Riihelä A 2024 Earth's sea ice radiative effect from 1980 to 2023 *Geophys. Res. Lett.* **51** e2024GL109608
[16] Marcianesi F, Aulicino G and Wadhams P 2021 Arctic sea ice and snow cover albedo variability and trends during the last three decades *Polar Sci.* **28** 100617
[17] Friedlingstein P *et al* 2026 Emerging climate impact on carbon sinks in a consolidated carbon budget *Nature* **649** 98–103
[18] Ke P *et al* 2024 Low latency carbon budget analysis reveals a large decline of the land carbon sink in 2023 *Natl. Sci. Rev.* **11** nwae367
[19] Gatti L V *et al* 2021 Amazonia as a carbon source linked to deforestation and climate change *Nature* **595** 388–93
[20] Brienen R J W *et al* 2015 Long-term decline of the Amazon carbon sink *Nature* **519** 344–8
[21] Séférian R, Bossy T, Gasser T, Nichols Z, Dorheim K, Su X, Tsutsui J and Santana-Falcón Y 2024 Physical inconsistencies in the representation of the ocean heat-carbon nexus in simple climate models *Commun. Earth Environ.* **5** 1–10
[22] Webb H *et al* 2025 A review of abrupt permafrost thaw: definitions, usage and a proposed conceptual framework *Curr. Clim. Change Rep.* **11** 7
[23] Brovkin V, Bartsch A, Hugelius G, Calamita E, Lever J J, Goo E, Kim H, Stacke T and de Vrese P 2025 Permafrost and freshwater systems in the Arctic as tipping elements of the climate system *Surv. Geophys.* **46** 303–26
[24] Turetsky M R *et al* 2020 Carbon release through abrupt permafrost thaw *Nat. Geosci.* **13** 138–43
[25] Deutloff J, Held H and Lenton T M 2025 High probability of triggering climate tipping points under current policies modestly amplified by Amazon dieback and permafrost thaw *Earth Syst. Dyn.* **16** 565–83
[26] Smith C J, Forster P M, Allen M, Leach N, Millar R J, Passerello G A and Regayre L A 2018 FAIR v1.3: a simple emissions-based impulse response and carbon cycle model *Geosci. Model Dev.* **11** 2273–97
[27] Millar R J, Nicholls Z R, Friedlingstein P and Allen M R 2017 A modified impulse-response representation of the global near-surface air temperature and atmospheric concentration response to carbon dioxide emissions *Atmos. Chem. Phys.* **17** 7213–28
[28] Wunderling N, Krönke J, Wohlfarth V, Kohler J, Heitzig J, Staal A, Willner S, Winkelmann R and Donges J F 2021 Modelling nonlinear dynamics of interacting tipping elements on complex networks: the pycascades package *Eur. Phys. J. Spec. Top.* **230** 3163–76
[29] Wunderling N, Winkelmann R, Rockström J, Loriani S, McKay D I A, Ritchie P D L, Sakschewski B and Donges J F 2023 Global warming overshoots increase risks of climate tipping cascades in a network model *Nat. Clim. Change* **13** 75–82
[30] Möller T, Högner A E, Schleussner C-F, Bien S, Kitzmann N H, Lamboll R D, Rogelj J, Donges J F, Rockström J and Wunderling N 2024 Achieving net zero greenhouse gas emissions critical to limit climate tipping risks *Nat. Commun.* **15** 6192
[31] Kriegler E, Hall J W, Held H, Dawson R and Schellnhuber H J 2009 Imprecise probability assessment of tipping points in the climate system *Proc. Natl Acad. Sci. USA* **106** 5041–6
[32] Steinert N J and Sanderson B M 2025 Normalizing the permafrost carbon feedback contribution to the transient climate response to cumulative carbon emissions and the zero emissions commitment *Earth Syst. Dyn.* **16** 1711–21
[33] Steinert N J 2025 normansteinert/PerCX: v1.0.1
[34] Meredith M *et al* 2022 Polar Regions *The Ocean and Cryosphere in a Changing Climate* (Cambridge University Press) pp 203–320
[35] Knoblauch C, Beer C, Liebner S, Grigoriev M N and Pfeiffer E-M 2018 Methane production as key to the greenhouse gas budget of thawing permafrost *Nat. Clim. Chang.* **8** 309–12
[36] Heslop J K, Winkel M, Anthony K M W, Spencer R G M, Podgorski D C, Zito P, Kholodov A, Zhang M and Liebner S 2019 Increasing organic carbon biolability with depth in yedoma permafrost: Ramifications for future climate change *J. Geophys. Res. Biogeosci.* **124** 2021–38
[37] MacDougall A H 2021 Estimated effect of the permafrost carbon feedback on the zero emissions commitment to climate change *Biogeosciences* **18** 4937–52
[38] Cui M, Ji D and Chen Y 2025 Permafrost response and feedback under temperature stabilization and overshoot scenarios with different global warming levels *Earth Syst. Dyn.* **16** 1809–31
[39] Yumashev D, Hope C, Schaefer K, Riemann-Campe K, Iglesias-Suarez F, Jafarov E, Burke E J, Young P J,

Elshorbany Y and Whiteman G 2019 Climate policy implications of nonlinear decline of Arctic land permafrost and other cryosphere elements *Nat. Commun.* **10** 1900

[40] Mengis N *et al* 2020 Evaluation of the University of Victoria earth system climate model version 2.10 (UVic ESCM 2.10) *Geosci. Model Dev.* **13** 4183–204

[41] Forster P *et al* 2021 The Earth's Energy Budget, Climate Feedbacks and Climate Sensitivity *Climate Change 2021 – The Physical Science Basis. Contribution of Working Group I to the Sixth Assessment Report of the Intergovernmental Panel on Climate Change* ed V Masson-Delmotte *et al* (Cambridge University Press) pp 923–1054

[42] Smith C *et al* 2021 The Earth's energy budget, climate feedbacks and climate sensitivity supplementary material *Climate Change 2021 – The Physical Science Basis. Contribution of Working Group I to the Sixth Assessment Report of the Intergovernmental 484 Panel on Climate Change* ed V Masson-Delmotte *et al* (Cambridge University Press) pp 923–1054

[43] Smith C J, Khourdajie A A, Yang P and Folini D 2023 Climate uncertainty impacts on optimal mitigation pathways and social cost of carbon *Environ. Res. Lett.* **18** 094024

[44] Ritchie P D L, Clarke J J, Cox P M and Huntingford C 2021 Overshooting tipping point thresholds in a changing climate *Nature* **592** 517–23

[45] Ritchie P D L *et al* 2026 The implications of overshooting 1.5 C on Earth system tipping elements–a review *Environ. Res. Lett.* **21** 043001

[46] Wunderling N, Donges J F, Kurths J and Winkelmann R 2021 Interacting tipping elements increase risk of climate domino effects under global warming *Earth Syst. Dyn.* **12** 601–19

[47] Weijer W, Cheng W, Drijfhout S S, Fedorov A V, Hu A, Jackson L C, Liu W, McDonagh E L, Mecking J V and Zhang J 2019 Stability of the atlantic meridional overturning circulation: a review and synthesis *J. Geophys. Res.: Oceans* **124** 5336–75

[48] Klose A K, Karle V, Winkelmann R and Donges J F 2020 Emergence of cascading dynamics in interacting tipping elements of ecology and climate *R. Soc. Open Sci.* **7** 200599

[49] Lenton T M et al 2025 The Global Tipping Points Report 2025 *Techinical Report* (University of Exeter)

[50] Natali S M, Holdren J P, Rogers B M, Treharne R, Duffy P B, Pomerance R and MacDonald E 2021 Permafrost carbon feedbacks threaten global climate goals *Proc. Natl Acad. Sci. USA* **118** e2100163118

[51] Schädel C *et al* 2024 Earth system models must include permafrost carbon processes *Nat. Clim. Chang.* **14** 114–6

[52] Schädel C, Gasser T, Rogers B M, Treharne R, Turetsky M R, Smith T, MacDonald E and Natali S M 2026 Permafrost and wildfire carbon emissions indicate need for additional action to keep Paris Agreement temperature goals within reach *Commun. Earth Environ* 1–11

[53] Steinert N J, Munday G, Sandstad M, Sanderson B M and Wunderling N 2026 Code for Permafrost carbon-climate feedback amplifies Earth system tipping risks (https://doi.org/10.6084/m9.figshare.31376533)